From Natural Complexity to Biomimetic Simplification: Realization of Bionic Fish Inspired by the Cownose Ray

Yueri Cai, Shusheng Bi, Guoyuan Li, *Member, IEEE*, Houxiang Zhang, *Senior Member, IEEE*, Hans Petter Hildre

***Abstract*—Features of fish like environmental compatibility and maneuverability have attracted bio-inspired design researchers worldwide to contemplate the practical applications of robotic fish. This paper presents a conceptual design and development of a robotic fish based on the cownose ray. We extracted essential biomimetic parameters of the cownose ray to develop reasonable simplifications of the body shape, the mechanical structure design principle of the multi-joint driving fin rays, and the motion principle. Practical motion abilities of the internal driven skeleton of the bionic prototype are calculated theoretically and compared with its natural model. Parameters affecting propulsion performances are analyzed utilizing a one-dimensional calculation method. The basic motion modes are obtained according to the analysis. Observations show that the developed robotic fish can perform bionic sinusoidal flapping movements. Positive forward propulsion forces and desired turn torques are measured on the towing tank. The maximum linear forward swimming speed of the bionic fish is 0.7 times of body length per second (BL/s). Maneuvering abilities of the pivot turn and swimming through narrow passages by rolling swim are demonstrated to confirm the design idea.**

***Index Terms*—bionic fish; cownose ray; swimming modes; flapping motion;**

I. Introduction

NOVEL types of underwater vehicles that feature environmental compatibility and maneuverability are in high demand nowadays. For example, underwater vehicles with low environment disturbance and biological similarity are advantageous for aquaculture. Fish-like underwater robots are promising responses to this problem [1]-[3]. It is clear that bionic fish, a novel kind of underwater robot, which would have many of the outstanding features of fish, offer distinct advantages. Researchers have already carried out beneficial explorations of the practical applications of bionic fish from the laboratory, such as in marine applications [2] and for science education [3].

Many fish turn using oscillating pectoral fins. These fins also play an important role in their ability to maneuver and their excellent stability [4], [5]. Some bionic prototypes have reproduced these excellent features to a certain extent [6], [7]. The cownose ray has flapping paired pectoral fins that provide greater efficiency and velocity than other elasmobranches with fluctuating pectoral fins [8]. This is mainly attributed to their pectoral fins' special low-frequency flapping movement and low-energy consumption gliding motion [9]. Given these advantages of the cownose ray, attention to bionic fish propelled by paired wide pectoral foils has been increasing [10], [11]. The bionic fish prototype demonstrated in this paper provides a biomimetic platform that has a potentially wide application in marine aquaculture. Fig. 1 shows one of the design concepts. The robotic prototype can be equipped with multiple sensors and devices for a wide range of applications, including the investigation and monitoring of water quality and sedimentation processes, inspection of fish farm nets and equipment, fish observations, and biomass estimation.

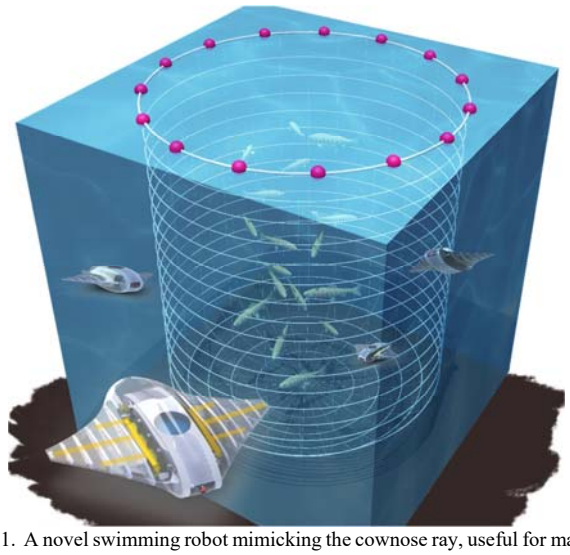

Fig. 1. A novel swimming robot mimicking the cownose ray, useful for marine aquaculture and environmental investigations.

Manuscript received March 20, 2018. This work is supported by Beijing Natural Science Foundation (No. 3182019).

Yueri Cai and Shusheng Bi are with the Robotics Institute, Beihang University (BUAA), Beijing 100191, China. Currently, Yueri Cai is taking postdoctoral research scholarship in Norwegian University of Science and Technology (NTNU), Norway, supported by China Scholarship Council (CSC). (e-mail: caiyueri@ buaa.edu.cn, yueri.cai@ntnu.no).

Guoyuan Li, Houxiang Zhang and Hans Petter Hildre are with Department of Ocean Operations and Civil Engineering, Norwegian University of Science and Technology (NTNU), Norway.

Researchers increasingly acknowledge, that specific fin shapes [12], body flexibility [13], [14], and complicated foil deformation [15] play important roles in the propulsion performance of bionic fish. Therefore, the bionic prototypes that use more complex mechanism, which are actuated by multiple fin rays, are developed accordingly [16], [17]. Through this kind of design, the bionic fish prototypes can mimic their counterparts in nature to a greater extent. It will promote the bionic research combined with functions and morphology. Although the structures and control method of this kind of bionic fish are very complicated, the advantages are obvious:

- It reproduces the driving waves of the cownose ray pectoral foil accurately.
- It can swim with low hydrodynamic noise, high efficiency, and environmental compatibility.
- It possesses main features of the natural sample, therefore reverse research can be carried out without real fish.

The practical performance of bionic fish depends on whether the design incorporates thorough insight into the structure discipline and propulsion mechanism of the natural fish, and whether we apply them properly in the bionic designs. The challenging issues in this procedure are how to extract key structure and movement parameters from the fish in nature, how to create an abstract practical model with feasible bionic simplifications, and how to design a physical bionic mechanism to fulfill the biomimetic requirements. Here, we introduce the systematic bionic design and development of a bionic fish to reproduce the typical structures and movements of the cownose ray.

II. Structure and Movement of Cownose Rays

As a typical species of eagle ray, the cownose ray has a skeleton inside its pectoral foil composed of hundreds of segmental cartilages. This structure means that with small range of movement of each segmental cartilage, the pectoral foil flaps widely. The bionic design will refer to this structure, but with some necessary simplifications. For example, dimensions of the cartilages are enlarged to accommodate the requirements of the bionic driving mechanism.

Dorsal shapes of the cownose ray's pectoral foil and body are extracted by setting markers on the edges of the cownose ray's picture in a direct overhead view. The actual shape of the right pectoral foil in dimensionless form is shown in Fig. 2(a). The coordinate values are non-dimensionalized by chordwise length of the fin base, i.e., by the maximum length of the pectoral foil along the chordwise direction involved in the flapping movements.

The spatial shape of the pectoral foil is another obvious characteristic that affects propulsion performance. Referring to the biologic anatomy of the cownose ray, as shown in Fig. 2(b), cross-sections along the chordwise direction of the cownose ray's pectoral foil can be approximated to a series airfoil shapes developed by the National Advisory Committee for Aeronautics (NACA), from NACA0020 to NACA0012, with gradient changes from the fin base to the fin tip.

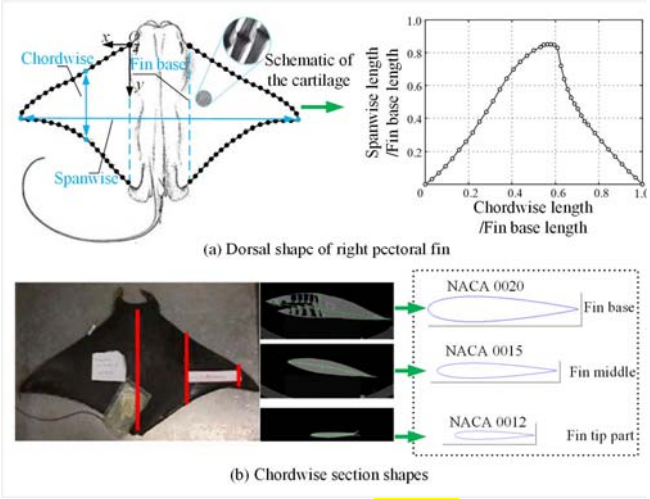

Fig. 2. Shape and structures of cownose ray [18], [19].

Using visual processing software we developed, we extract the movement disciplines of the cownose ray's special "mobuliform" motion in different swimming modes. Fin tip, fin base, leading edge, and trailing edge of the sample cownose ray's pectoral foil are selected as the key points or lines. Snapshots of a typical flapping cycle of a sample cownose ray in linear forward swim are shown in Fig. 3(a). Key movement features of cownose ray can be summarized as follows:

- The pectoral foil flaps with frequencies varying from 0.4 Hz to 1.2 Hz, changing with the swim conditions. Frequencies between 0.5 Hz and 0.6 Hz are usually used in linear forward swim.
- Foil deformation in flapping movements is consistent with sinusoidal discipline, especially along the chordwise direction.
- There are about 0.4 driving waves passing on the pectoral foil along the chordwise direction.
- The flapping amplitude of the cownose ray's pectoral foil is as large as half of the fin base length.

The cownose ray has many different swim modes to handle complicated underwater environments. The typical modes are linear forward swim, turn, up-floating, and diving. Series snapshots of some of the modes are shown in Fig. 3(a), Fig. 3(b), and Fig. 3(c). As well, when meeting obstacles such as reefs, seaweed, or predators, cownose rays will merge different swimming postures to realize a quick turn or a rolling swim. All the swimming modes required are realized by its large, flat pectoral foils and its flexible body, which are attributed to the complex biological structures of the ray's flexible cartilage, muscles and body. The natural characteristics are too complicated for a manufactured mechanism to replicate at this stage. The design thus has some simplifications, but seeks to approximately duplicate the cownose ray's outstanding swim performance by reproducing its key characteristics.

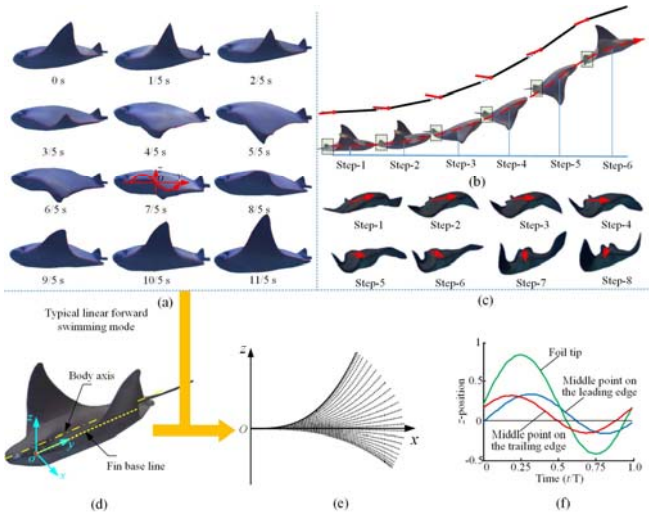

Fig. 3. Motion discipline analysis of the cownose ray. (a) linear forward swimming mode; (b) up-floating movement; (c) highly maneuvering swim; (d) the coordinate system setting; (e) flapping motion along spanwise direction; (f) sinusoidal movement along chordwise direction.

Here, we choose the typical linear forward swim mode to derive the simplified motion discipline that will be utilized to direct the design of the bionic fish. As shown in Fig.3 (d), the origin point of the coordinate system is set on the intersection point of the pectoral foil leading edge and the foil base line. The *x*-axis is paralleled with the lateral body axis and points to the tail direction, the *y*-axis is along the spanwise direction, and the *z*-axis is parallel with the dorsal ventral body axis.

For each cross section along the spanwise direction on the pectoral foil, the flapping movements in a cycle are simplified to oscillation of series curves. At each time step, the curve is consistent with a kind of cubic curve with specific coefficients, as shown in Fig. 3(e). All the spanwise sections are supposed to employ the same motion discipline. Only the phase differences and the amplitudes are different, due to the chordwise position, i.e., the value of coordinate *y* shown in Fig. 3(d), and the triangle shape of the pectoral foil. For chordwise cross sections, sinusoidal waves pass along the *y*-axis from head to tail, with identical wavelength and frequency. Motion curves of the key points, i.e., the middle point on the leading edge and the trailing edge, and the foil tip point, are shown in Fig. 3(f). It can be observed that there is 0.1T phase difference between each two adjacent key points. This phase difference generates 0.4 waves passing on the pectoral foil in steady linear forward swim. The principle is consistent with the biological analysis results of the cownose ray [28]. Considering the practical design requirements for vertical motion balance, the difference between the upper flapping amplitude and the lower flapping amplitude are omitted in our design at this stage. If we designed a bionic prototype with different upstroke and downstroke amplitudes, it would be difficult to control the motion depth of the bionic fish, and the dynamic deformation of the pectoral foil would have to be more complicated. Therefore, influence of the kind of motion is set as one of our future research objectives.

III. Bionic Fish Design

The mechanism of the designed inside skeleton shown in Fig. 4 is applied to mimic the pectoral foil movement deformation of the cownose ray. Each side of the inside skeleton is composed of three fin rays uniformly distributed at the fin base along the chordwise direction. These fin rays play the key propulsive role. A one-stage slider-rocker mechanism is applied to the front fin ray. A two-stage slider-rocker mechanism is utilized for the middle fin ray. The rear fin ray is made of a well-cut flexible carbon fiber plate with a special designed shape, based on the analysis before. It is driven by the servo motor directly, without a transmission mechanism. As can be seen in Fig. 4(a), there are two fin rays located at the tail part of the middle body. The tail fin rays function like lift rudders, assisting the pectoral foils in floating and submerging. At each time step, the optimized slider-rocker mechanism is verified to fit the spanwise flapping cubic curves extracted from the cownose ray with minimized errors.

Practical motion of every point on the bionic pectoral foil is a compound movement withspanwise flapping motion and chordwise sinusoidal wave transmission. . The driving laws applied to the servo motors of the front fin ray, the middle fin ray, and the rear fin are shown in Fig. 4(b). In terms of the design, this driving law follows a cownose ray to generate the desired driving waves.

The rear fin ray uses only one linkage; therefore it will duplicate the reciprocating movement of its servo motor. As discussed before, the middle fin ray uses the two-stage slider-rocker mechanism and the front fin ray uses a one-stage mechanism. If the middle fin ray can achieve the required motion, the front fin ray will follow the same rules. Therefore, the middle fin ray is taken as an example to estimate the feasibility of the motion. As shown in Fig. 4(a), three key points, i.e., the two rotating joints and the fin tip, are taken as the targets. Motion curves calculated in a full flapping cycle for all the three points selected are shown in Fig. 4(c). It can be seen that motions of all the three key points oscillate in phase with a high level of sinusoidal curves and approximate to the flapping discipline of cownose ray's pectoral foil. There is limited movement error between the designed slider-rocker mechanism and the curve from cownose ray at each time step.

The physical bionic fish is composed of two main parts, the outer skin-like cover and the inside driving skeleton. The inside skeleton shown in Fig. 5(a) possesses functions of propulsion and supporting the outer appearance shape. The middle body is a waterproof box made of aluminum plates and plexiglass. Battery, control circuits, driving board, and communication apparatus are placed in the middle body. Each fin ray, including the two at the tail part, is driven by an independent high torque servo. All the servos are covered by a single sealing box to make them water-isolated. The middle body and the sealing box are filled with compressed air of 0.1 MPa to test the sealing conditions and strengthen pressure resistance capability of the middle body and the sealing boxes.

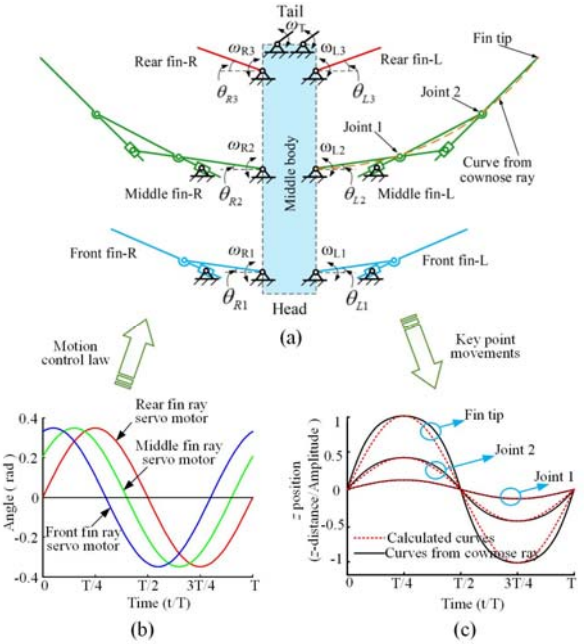

Fig. 4. Kinematic analysis of the designed inside skeleton. (a) mechanism of the inside skeleton; (b) driving laws applied; (c) movement of the key points.

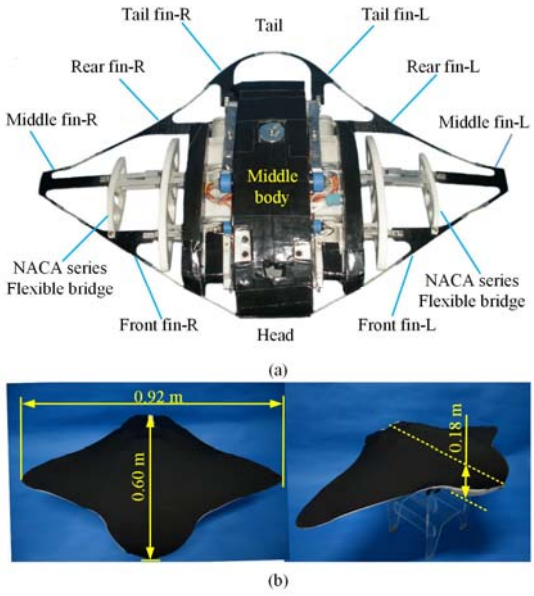

Fig. 5. Internal skeleton structure of the bionic fish without counterbalancing parts and the outer skin.

The outer shape of the tip linkage of each fin ray fits the corresponding shape profile of the reference cownose ray. The tip linkages are made of carbon fiber plates with thickness of 1 mm, to ensure both elasticity and support ability of the outer edges. Flexible bridges connecting the front fin ray and middle fin ray are designed to support the chordwise spatial shape. They can assist in realization of the smooth foil flapping and passing wave continuity along the chordwise direction. The bridges are formed by room-temperature-vulcanization double component silicon rubber. Their dimensions, including width and thickness distributions, are decided according to the requirements of realizing passive flexible deformation of the pectoral foil tip parts, as well as smooth deformation of the covering skin between each two neighboring fin rays. The inside skeleton is strengthened to endure water pressure and counterbalanced after sealing work finished. The outer flexible skin of the bionic fish is made of pervious nylon cloth with outstanding elasticity of about 1.5 to 2 times of tensile ability. During the consecutive motion combined by the fin rays, the bridges, the outer skin, and other supporting parts, the outer skin can fill the structure gaps and make the movement smoother.

After second-step counter-balancing, the prototype can suspend in water without any movements. Basic mechanical parameters of the bionic fish are shown in Fig. 5(b). Total mass of the prototype is 6.2 kg after balance. The size and morphology are very similar to the cownose ray in nature.

IV. Propulsion and Posture Analysis

It is clear that swimming modes of the developed bionic fish can be actively adjusted by changing the flapping amplitude, the frequency, and the phase differences, etc. Propulsion forces generated by the bionic pectoral foils change along with these parameters as well as the different swim postures.

We evaluate the propulsion force production capability of the bionic fish prototype developed theoretically by applying a one-dimensional calculation method here. Based on the motion law extracted from cownose ray, each chordwise cross-section on the pectoral foil employs the same kind of movement that is consistent with sinusoidal discipline, referring mainly to flapping frequency and wavelength. Only the amplitudes change with different spanwise positions. Therefore, the flapping foil can be taken as a one-dimensional flexible foil, which can be used to calculate influences of the key parameters on the propulsion force performance.

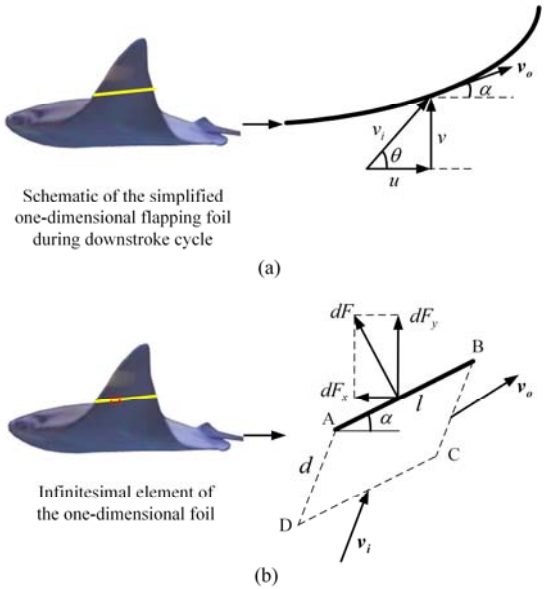

Fig. 6. Schematic of one-dimensional analysis method of a linear forward swim cownose ray: (a) model of the one-dimensional flapping foil; (b) force model on the infinitesimal element.

Considering value of the Reynolds number of the bionic fish at this dimension and swim conditions, we omit the influence of the viscous force in calculations here. The coordinate system settled in Fig. 3(d) is employed once again. An instantaneous position of the one-dimensional pectoral foil is taken as the analysis target here, as the yellow line shown in Fig. 6(a). According to the foregoing analysis of the cownose ray, all the parts of the pectoral foil oscillate with the same sinusoidal discipline. The simplified pectoral foil obeys the same law.

The flapping movements and the induced velocity generated by the pectoral foil can be stated by:

$$h(t) = h_0 \cos(\omega t) \tag{1}$$

$$v(t) = -\dot{h}(t) = h_0 \omega \sin(\omega t) \tag{2}$$

where, h_0 represents the flapping amplitude of the pectoral foil and ω represents the angular frequency. Then, as shown in Fig. 6(a), the practical velocity relative to the coming flow can be deducted, which is vector sum of the movement velocity $\boldsymbol{v}$ and the incoming flow velocity $\boldsymbol{u}$:

$$\boldsymbol{v}_i = \boldsymbol{u} + \boldsymbol{v} \tag{3}$$

The force condition of each infinitesimal element on the simplified pectoral foil is shown in Fig. 6(b). The infinitesimal element is sufficiently small that it can be treated as a linear segment. For a short variable time Δt, the infinitesimal element sweeps out an area of

$$\Delta S = v_i \Delta t l \sin(\theta - \alpha) \tag{4}$$

where, l represents length of the infinitesimal element, θ is the included angle between the movement velocity and the incoming flow, and α is the angle of attack. Therefore, the liquid mass swept by the infinitesimal element is:

$$\Delta m = \rho \Delta S = \rho l \Delta t (v \cos\alpha - u \sin\alpha) \tag{5}$$

Then, based on the momentum theorem, the force perpendicular to the infinitesimal element can be calculated:

$$dF = \frac{\Delta m v_{in} - \Delta m v_{on}}{\Delta t} \tag{6}$$

where v_{in} represents normal component of the inflow velocity and v_{on} represents the normal component of the outflow velocity. The liquid flow that cannot cross the infinitesimal element. After interacting with the element, it translates to a tangential direction parallel to the element. Therefore, v_{on}=0in equation (6). Then, the force perpendicular to the element generated by the inflow velocity can be obtained. The propulsion force generated by the entire simplified pectoral foil is:

$$F_x = \int \rho l (v \cos\alpha - u \sin\alpha)^2 \sin\alpha dl \tag{7}$$

In an entire flapping cycle, equation (7) can be simplified to

$$F_x = \rho \bar{c} (h_0 \omega \sin(\omega t) \cos\bar{\alpha} - u \sin\bar{\alpha})^2 \sin\bar{\alpha} \tag{8}$$

where $\bar{\alpha}$ represents the average pitching angle of all the infinitesimal elements subdivided by the simplified one-dimensional foil, and $\bar{c}$ represents average chord length of the pectoral foil.

We can utilize equation (8) to discuss conditions that produce the propulsion forces. According to the movement discipline extracted from cownose ray, whether the pectoral foil flaps upstroke or downstroke, the value of the average pitching angle is always between 0 and $\pi/2$. This means that the pectoral foil can produce positive propulsion force in both flapping directions. Some qualitative regularities can be deduced accordingly.

First, both the flapping amplitude and the pitching angle have obvious positive effects on the generation of the propulsion force. This means that if we apply the larger of these two parameters, it will produce the higher propulsion force, within the mechanical structure limitations. Second, since there are three fin rays placed along chordwise direction at each pectoral foil and each fin ray can be controlled independently, the phase difference between each two neighboring fin rays will be settled as positive or negative. This means that direction of the driving waves passing on the pectoral foil can be controlled. The waves have significant influences on the propulsion forces. For example, if the driving wave transmits from tail to head, adverse to the usual direction applied, the direction of the propulsion force will point to the tail. Different combinations mean different swim modes. Fig. 15 shows typical swim modes of the bionic fish that can be achieved through properly arranging the variable parameters.

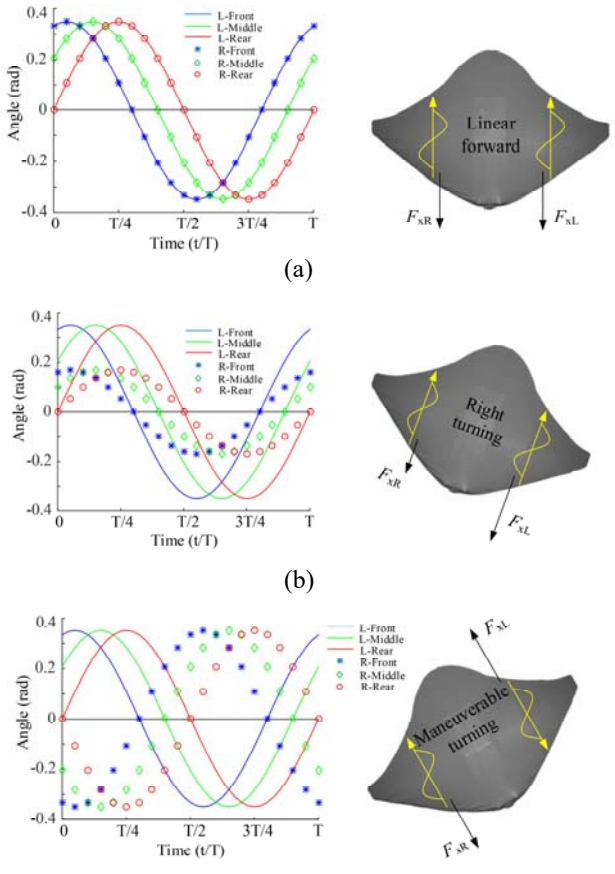

Fig. 7. Typical swim postures of the bionic fish and corresponding transmission conditions of the driving waves: (a) linear forward swim; (b) ordinary turn; (c) high maneuvering turn. L denotes the left pectoral fin, R denotes the right pectoral fin.

- Linear forward swim. Identical control parameters are applied to each symmetric pair of the fin rays. The two pectoral foils produce equal forward thrust.
- Ordinary turn. The pectoral foil at the target side employs lower value parameters. The turning movement can be achieved by the different forward propulsion force generated. The bionic fish will turn with a non-zero radius.
- Highly maneuverable turn. The two pectoral foils flap with equal amplitude and frequency, but with completely opposite phase difference. A nearly pure turning torque is imposed on the bionic fish.

The bionic fish realizes floating or diving motion by its two tail fin rays. Theoretically, the bionic fish can realize all the basic movements, owing to the bionic multiple fin ray driving system.

V. Experimental Results

A. Posture Observations

In the observation, the prototype is fixed to a frame above the water tank through a rod connected at its upper head point, as shown in Fig. 8(a). The water depth fulfills requirements that the bionic fish can be fully submerged in water during the entire flapping cycle. We put six uniformly distributed observation markers on the edge of each pectoral foil: three markers are on the leading edge and the other three on the trailing edge, as can be seen in Fig. 8(a) and (c). The experimental settings are illustrated in Table I. The tail part of the bionic fish employs simple oscillatory movements as shown in Fig. 8(b). It swings with fixed angles and performs as an elevator. In Fig. 8(a), successive snapshots of the bionic fish flapping in a typical linear forward swim in a full flapping cycle are shown, seen from the lateral view. Large flapping amplitude and obvious pitching movement can be observed, as a result of the controllable driving waves passing on the pectoral foil.

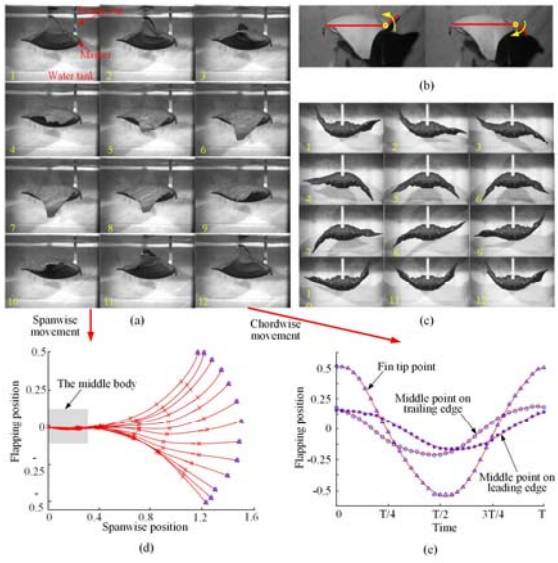

Fig. 8. Experiments for observing motions of the bionic fish. (a) the experimental setups and the linear forward swim; (b) movement of the tail fin; (c) highly maneuvering turn; (d) flapping motion along spanwise direction; (e) sinusoidal movement along chordwise direction.

TABLE I
Experimental Settings

Camera model	FastCam 1280 PCI
Camera speed rate (fps)	120
Shutter time (s)	1/500
Flapping frequency (Hz)	0.6
First linkage flapping amplitude (deg.)	20
Phase difference of adjacent fin rays (T)	0.1

Profile variations during downstroke cycle of the leading edge of the right pectoral foil in typical linear forward swim are extracted. Clear flapping movements in line with series cubic-curves that observed from the cownose ray are achieved. Fig. 8(e) shows the chordwise motion tracking results of the markers settled. Practically, the three mark points employ equal flapping frequency and wavelength; the only difference is flapping amplitude caused by the different spanwise positions. Phase difference between each two neighboring fin rays is about 0.12 s. This phenomenon is collectively caused by transmission performance of the mechanical system, rigidity of the flexible bridge shown in Fig. 5(a), pulling force from the outer covering skin, and influence of hydrodynamic force.

As discussed previously, when the high maneuvering turn is carried out, the pectoral foils employ the most complicated postures. In Fig. 8(c), full cycle snapshots of the high maneuvering turn of the prototype seen from the front view are shown. The movements are consistent with which is designed in Fig. 7(c). From these observations, it can be concluded that the typical motion modes of the cownose ray can be obtained by the bionic fish.

B. Force Measurement

Propulsion force and turning torque produced by the paired pectoral foils, referring to different flapping postures, are obtained through tests in another water tank. The water tank used is 5 m in length and 3 m in width. The water depth used is 0.6 m. The bionic fish prototype is placed at a position with distance of 0.3 m to the water surface. The fixing method is similar to that in posture observation experiments. The connecting point at the head part of the bionic fish is fixed to a 6-axis force sensor. Flapping frequency of 0.5 Hz and flapping angle of 16 degrees are applied to the servo motors. The phase difference between two neighboring fin rays is set to 0.1 T. For the ordinary turn here, the limited posture is utilized, i.e., the pectoral foil at the target direction is kept still at the median position and the other pectoral foil flaps using planned parameters.

Instantaneous values of thrust and turning torque of the bionic fish at typical swim postures are shown in Fig. 9.

- Linear forward swim. Equal time positive propulsion force and negative propulsion force are generated. By contrast, absolute values of the positive forces are higher. Then, resultant forward force is obtained eventually. Turning torque fluctuates at high frequency with limited values.
- Ordinary turn. The positive torques last longer and in a

movement cycle the positive propulsion force produced is higher, with smaller value difference than that in linear forward swim. It means that the bionic fish will turn and swim forward at the same time.

- High maneuvering turn. The average forward propulsion force is around zero. Almost pure torque is applied. It means that the forward movement will be limited when the bionic fish turns.

The maximum and the average values of forward thrust and turning torque at different flapping modes are summarized in Table II. The average absolute values are all obtained from ten full cycles of flapping movements in the experiments.

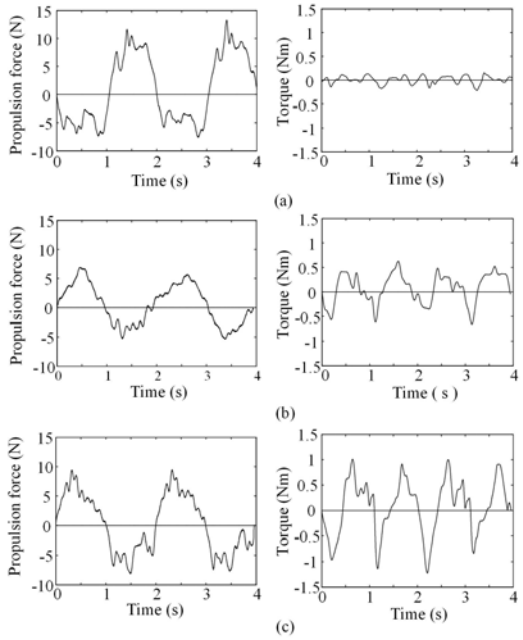

Fig. 9. Instantaneous thrust and turning torque of the bionic fish at different movement postures: (a) typical linear forward swim; (b) ordinary turn; (c) high maneuvering turn.

TABLE II
FORCE TORQUE OF DIFFERENT POSTURES

Postures	Linear forward swim	Ordinary turn	High maneuvering turn
Maximum Thrust (N)	13.42	6.80	10.51
Average Thrust (N)	0.90	0.55	0.13
Maximum Turning Torque (Nm)	0.21	0.62	1.32
Average Turning Torque (Nm)	0.02	0.07	0.08

Absolute values appear in this table.

C. *Swim Performance*

Practical swimming tests show that the desired smooth underwater swim can be reached. Flexible deformation of the pectoral foil is strengthened and the unsmooth connection occurred on the leading edge at the gap between each two neighboring fin rays is decreased, because of the action of the flexible and stretchable outer skin. Snapshots of the bionic fish prototype swims in the water tank, in its two amplitude positions, are shown in Fig. 10(a). It obtains large flapping amplitudes, much like the cownose ray.

The maximum linear forward swim velocity obtained by the bionic fish is about 0.42 m/s, equal to 0.7 BL/s. As shown in Fig. 10(b), consecutive postures of a full cycle pivot turn are shown. Completely opposite phase differences are applied to the two pectoral foils here.

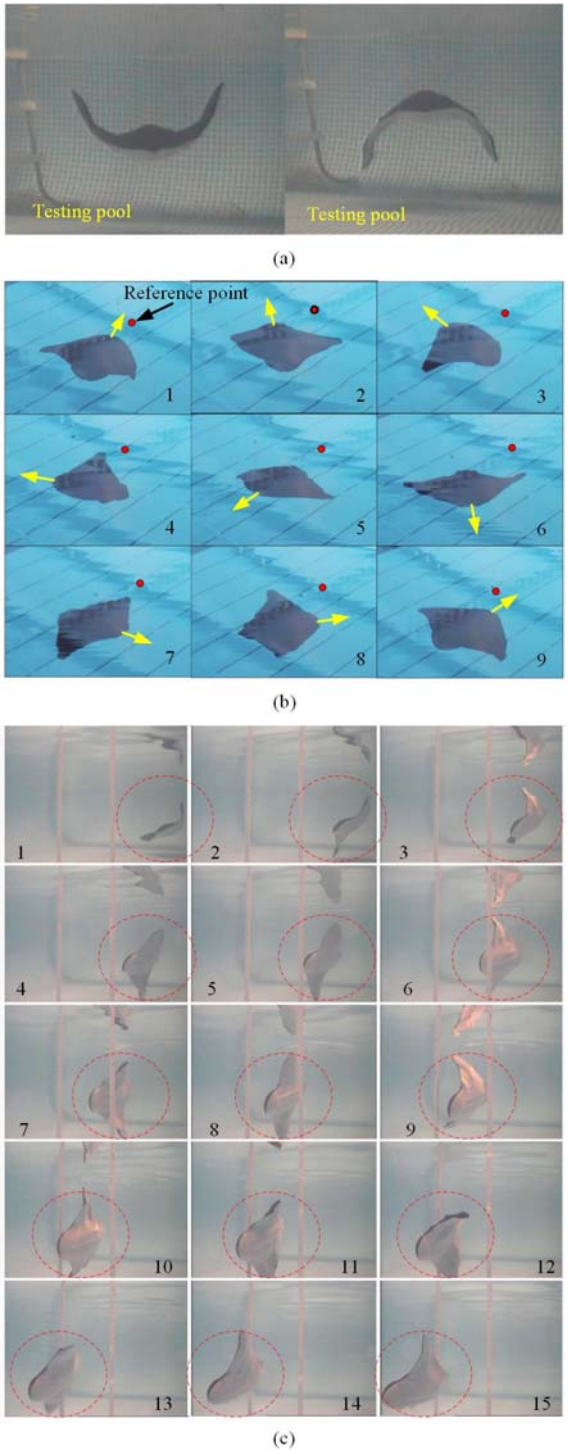

Fig. 10 Swim performance of the bionic fish. (a) linear forward swim; (b) highly maneuvering turn; (c) high maneuverability by roll swimming through a narrow passage.

The developed bionic fish possesses high maneuverability, which can also be illustrated by its tilting swim through a narrow passage. The continuous screenshots in water tank experiments are shown in Fig. 10(c). In the experiment, we send target roll angles to the bionic fish in real time by the installed wireless serial port, combined with opportune heading control. Two sticks are settled parallel to each other at a distance of 0.45 m to constitute the experimental narrow passage. As the former section illustrates, the thickest part of the bionic fish at the middle body is 0.18 m and the wing span of it is 0.92 m. By means of this special posture with a rolling angle of approximately 90 degrees, the bionic fish prototype can swim through narrow passages with width a little less than half of its wingspan.

VI. Conclusion and Ongoing Research

This paper has illustrated a novel bionic fish mimicking cownose ray with wide flat pectoral foils and discussed the prototype theoretically and experimentally. The bionic fish achieved self-driven capability and excellent maneuverability. It is suitable for underwater applications requiring high payload capability and maneuverability. It will be particularly useful in challenging environments like shallow water near the seaboard or water with lots of aquatic plants, due to its bionic structure and maneuverability.

The structure and shape of the cownose ray were analyzed based on the biology and anatomy research results, including the fin shape, the cross-sections, and the skeleton characteristics. Pectoral foil movement characteristics and flexible body deformation of a free-swimming cownose ray at different swim modes are summarized. Considering the design feasibility, both the structures and the movements of the cownose ray are simplified to fulfill the biomimetic development requirements. The irregular chordwise cross-sections are regularized to series NACA airfoil shapes. The complex skeletons composed of cartilaginous and flexible connections are simplified to a combination of multiple joint fin rays and flexible chordwise bridges. The complex movement deformation of the cownose ray is split up into two main components of chordwise wave transmission and spanwise flapping movement. Through these simplification methods, the bionic mechanism expressed in this paper can fulfill movement requirements of the bionic fish to ultimately meet the development targets.

Future tests and improvements of the bionic fish will be carried out. Sensors such as a gyroscope and depth sensor will be equipped and fully explored for autonomous swimming, infrared sensors for obstacle avoidance, etc., to make the bionic fish more adaptive to practical aquaculture applications.

Although the simplifications applied to bionic design can accelerate the development process, it is clear that the complex structures of cownose ray play important roles in the optimized performance of the bionic fish. Further investigations on the bionic fish prototype using soft materials are in progress. The prototype will provide movement functions and morphology following its natural model to a much greater extent.

Acknowledgment

The authors appreciate the support of the China Scholarship Council (CSC).

References

[1] J.Z. Yu, M. Wang, M. Tan, and J.W. Zhang, “Three-dimensional swimming,” *IEEE Robotics & Automation Magazine*, vol. 18, no. 4, pp. 47-58, 2011.

[2] Y.S. Ryuh, G.H. Yang, J.D. Liu, and H. Hu, “A school of robotic fish for mariculture monitoring in the sea coast,” *Journal of Bionic Engineering*, vol. 12, pp. 37-46, 2015.

[3] P. Phamduy, R. LeGrand, and M. Porfiri, “Robotic fish: Design and characterization of an interactive iDevice-Controlled robotic fish for informal science education,” *IEEE Robotics & Automation Magazine*, vol. 22, no.1, pp. 86-96, 2015.

[4] J.E. Harris, “The role of the fins in the equilibrium of the swimming fishII: The role of the pelvic fins,” *Journal of Experimental Biology*, vol. 13, pp. 476-493, 1938.

[5] H. Suzuki, N. Kato, K. Suzumori, “Load characteristics of mechanical pectoral fin,” *Experiments in Fluids*, vol. 44, no. 5, pp. 759-771, 2007.

[6] A. Asnafi, “A method to investigate general optimal maneuvers for kinematically reducible robotic locomotion systems,” *Journal of Intelligent and Robotic Systems*, vol. 84, pp. 799-813, 2016.

[7] Z.G. Zhang, N. Yamashita, M. Gondo, M. Yamamoto, and T. Higuchi, “Electrostatically actuated robotic fish: Design and control for high-mobility open-loop swimming,” *IEEE Transactions on Robotics*, vol. 24, no. 1, pp. 118-129, 2008.

[8] L.J. Rosenberger, “Pectoral fin locomotion in Batoid fishes: Undulation versus oscillation,” *The Journal of Experimental Biology*, vol. 204, 379-394, 2001.

[9] P.W. Webb, “Kinematics of plaice, Pleuronectes platessa, and cod, Gadus morhua, swimming near the bottom,” *The Journal of Experimental Biology*, vol. 205, pp. 2125-2134, 2002.

[10] Y.R. Cai, S.S. Bi, and L.C. Zheng, “Design and experiments of a robotic fish imitating cownose ray,” *Journal of Bionic Engineering*, vol. 7, no. 2, pp. 120-126, 2010.

[11] C.M. Chew, Q.Y. Lim and K.S. Yeo, “Development of propulsion mechanism for robot manta ray,” in *Proceedings of the 2015 IEEE Conference on Robotics and Biomimetics (ROBIO)*, Zhuhai, China, December 6-9, 2015, pp.1918-1923.

[12] B. Liu, Y.K. Yang, F.H. Qin, and S. W. Zhang, “Performance study on a novel variable area robotic fin”, *Mechatronics,* vol. 32, pp. 59-66, 2015.

[13] S. Heathcote, Z. Wang, and I. Cursul, “Effect of spanwise flexibility on flapping wing propulsion,” *Journal of Fluids and Structure*, vol. 24, pp. 183-199, 2008.

[14] A.K. Kancharala and M.K. Philen, “Optimal chordwise stiffness profiles of self-propelled flapping fins,” *Bioinspiration & Biomimetics*, vol. 11, 056016, 2016.

[15] A.I. Mainong, A.F. Ayob, and M.R. Arshad, “Investigating pectoral shapes and locomotive strategies for conceptual designing bio-inspired robotic fish,” *Journal of Engineering Science and Technology*, vol. 12, no. 1, pp. 001-014, 2017.

[16] C.L. Zhou and K.H. Low, “Better Endurance and Load capacity: An Improved Design of Manta Ray Robot (RoMan-II),” *Journal of Bionic Engineering*, vol. 7, Supplement 1, pp. S137-S144, 2010.

[17] S.W. Zhang, B. Liu, L. Wang, Q. Yan, K. H. Low, and J. Yang, “Design and implementation of a lightweight bioinspired pectoral fin driven by SMA,” *IEEE/ASME Transactions on Mechatronics*, vol. 19, no. 6, pp. 1773-1785, 2014.

[18] C.E. Heine, “Mechanics of flapping fin locomotion in the cownose ray, Rhinoptera bonasus (Elasmobranchii: Myliobatidae),” Ph. D dissertation, Department of Zoology, Duke University, Durham NC, USA, 1992.

[19] W. Huang, W. Hongjamrassilp, J.Y. Jung, P.A. Hastings, V.A. Lubarda, and J. McKittrick, “Structure and mechanical implications of the pectoral fin skeleton in the Longnose Skate (Chondrichthyes, Batoidea),” *Acta Biomaterialia*, vol. 51, pp. 393-407, 2017.